

Ultrasonic evaluation of polyether ether ketone and carbon fiber-reinforced PEEK

David A. Fitch · Brent K. Hoffmeister ·
Javier de Ana

Received: 18 November 2009 / Accepted: 18 March 2010 / Published online: 2 April 2010
© Springer Science+Business Media, LLC 2010

Abstract Polyether ether ketone (PEEK) and carbon fiber-reinforced (CFR) PEEK are commonly used in medical implants. This study evaluated the mechanical moduli of PEEK and CFR PEEK using nondestructive, ultrasonic tests. The Young's modulus of CFR PEEK was determined in all the spatial directions. Ultrasonic attenuation has not been studied extensively in PEEK, and not at all in CFR PEEK. The broadband ultrasound attenuations (BUAs) were determined for PEEK and CFR PEEK. The average Young's modulus, shear modulus, bulk modulus, and Poisson's ratio of PEEK were 4.21, 1.52, 6.25, and 0.388 GPa, respectively. The maximum and minimum Young's moduli of CFR PEEK were 15.1 and 5.1 GPa measured parallel and perpendicular to the fiber axis respectively. The longitudinal and transverse BUAs of PEEK were 1.33 and 4.37 dB/cm MHz, respectively. The longitudinal BUAs of CFR PEEK parallel and perpendicular to the fiber axis were 2.43 and 1.45 dB/cm MHz, respectively. Characterization of Young's modulus of CFR PEEK in all the spatial directions is useful for stiffness matching in implant design. The BUA values are useful in modeling the interaction of ultrasound and the PEEK materials and can also be used for developing non-destructive tests to find structural defects in implants made from these materials.

Introduction

Polyether ether ketone (PEEK) is a versatile polymer that has been increasingly used in biomedical applications over the last 20 years. PEEK has been used in trauma, spinal, and reconstructive implants because of its excellent biocompatibility, stability at high temperatures, radiolucency, and stability of mechanical properties when sterilized using Gamma radiation, steam, or ethylene oxide (EtO) [1, 2].

The mechanical properties of PEEK can be modified by infusing the material with reinforcing agents, such as carbon fibers. The mechanical properties of carbon fiber-reinforced PEEK (CFR PEEK) can be adjusted by varying fiber length, orientation, and concentration. The ability to adjust mechanical properties is useful in implant design when trying to match the stiffness of the implant and biological tissues, such as cortical bone. By knowing the mechanical moduli of CFR PEEK for every fiber orientation, designers can select which fiber orientation will meet their needs. This study will report mechanical moduli for CFR PEEK measured using ultrasonic techniques.

In addition, the ultrasound attenuations of both PEEK and CFR PEEK were studied. The ultrasound attenuation of PEEK has not been studied extensively, and a literature search yielded no reported values for CFR PEEK. These values are useful when modeling heating of implants due to exposure to ultrasound. Used in conjunction with speed of sound values of PEEK and CFR PEEK, these values may also be useful in developing nondestructive tests for finding structural defects in implants made from the materials. This study will examine the broadband ultrasound attenuations (BUAs) of longitudinal waves for PEEK and CFR PEEK. BUAs for transverse waves are investigated for PEEK as well.

D. A. Fitch · J. de Ana (✉)
Biologics and Spine, Smith & Nephew, Inc, Memphis, TN, USA
e-mail: javier.deana@smith-nephew.com

B. K. Hoffmeister
Department of Physics, Rhodes College, Memphis, TN, USA

Methods

Sample preparation

Seven PEEK samples were obtained by cutting a 6-mm diameter PEEK Optima[®] LT1 rod (Invibio Ltd., Thornton-Cleveleys, UK) into 5-mm sections. The CFR PEEK samples were cut from seven dog-bone-shaped PEEK Optima[®] LT1CA30 tensile bars with a cross section of 4 mm by 10 mm, and a parallel length of 60 mm before the bar begins to taper. The tensile bars had 30% by mass carbon fibers flow distributed along the long axis of the sample. Three samples were cut from the center of each tensile bar with nominal dimensions of 10 mm by 10 mm, 10 mm by 20 mm, and 5 mm by 10 mm (Fig. 1). These samples were called samples A, B, and C, respectively. Another sample, approximately 7 mm by 7 mm, was also cut from the center of the dog bone so that the sample had a fiber orientation of 77° with respect to the long axis of the sample. These samples were referred to as sample D. The surfaces used for ultrasonic measurements were machined to be flat and parallel. The density, ρ , of each sample was calculated by dividing the mass by the volume.

Speed of sound measurements

PEEK speed of sound measurements

Longitudinal couplant (Sonotech, Bellingham, WA) was applied to one end of a PEEK sample. The sample was

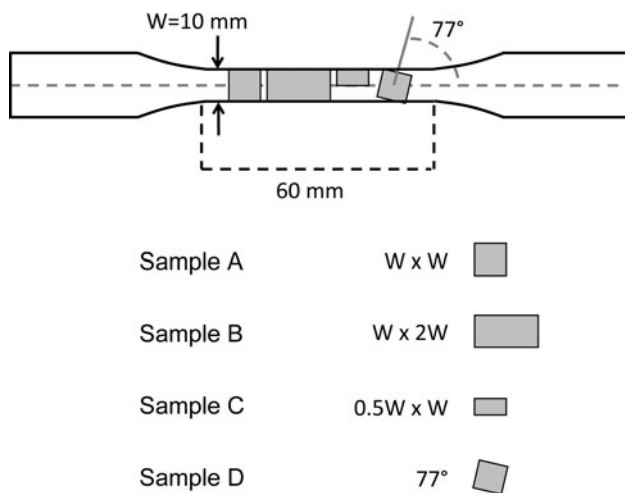


Fig. 1 Four samples were taken from the center of each CFR PEEK tensile bar. Sample A was 10 mm by 10 mm. Sample B was 10 mm by 20 mm. Sample C was 5 mm by 10 mm. Sample D was approximately 7 mm by 7 mm and prepared at a 77° angle relative to the long axis of the dog-bone specimen as shown. The dashed line through the center of the sample indicates the direction in which the fibers are assumed to be aligned due to the flow alignment of the fibers during the injection molding process

pressed firmly against a 5-MHz, 3-mm diameter longitudinal transducer (V1091, Olympus NDT, Waltham MA) connected to a pulser–receiver (5702PR, Olympus NDT, Waltham MA) operating in pulse–echo mode. The main bang and the first two echoes were captured and saved (Fig. 2a). The speed of sound, C , was calculated using Eq. 1, where t_0 and t_1 are the times at the start of the main bang and the first echo (Fig. 2a), and d is the length of the sample (Fig. 2b).

$$C = \left(\frac{t_1 - t_0}{2d} \right) \tag{1}$$

The PEEK sample was wiped clean, and shear couplant (Sonotech, Bellingham, WA) was applied to the sample. The sample was placed on a 5-MHz, 3-mm diameter shear transducer (V157-RM, Olympus NDT, Waltham MA) connected to the pulser–receiver in pulse–echo mode. The main bang and the first echo were captured and saved. The speed of sound was calculated in the same manner described above. Both the longitudinal, C_L , and transverse speed of sound, C_T , values were calculated for all the PEEK samples. The acoustic impedance, Z , was calculated as the product of ρ and C_L . Each of the seven PEEK samples was measured twice. After the first measurement, the transducer was moved to the opposite face of the specimen for the second measurement. The couplant was carefully removed and reapplied between measurements.

CFR PEEK speed of sound measurements

The speed of sound notation for these measurements is C_{yz}^x , where x is the propagation direction of the wave with respect to the fiber orientation, y indicates if the wave is longitudinal (L) or transverse (T), and z is polarization direction with respect to the fibers. Longitudinal couplant was applied to sample A from each dog-bone specimen. Each sample was placed on the longitudinal transducer so that the signal propagated parallel to the fiber orientation (Fig. 3a). The main bang and first echo were captured, and the longitudinal speed of sound parallel to the fiber orientation, $C_{L||}$, was calculated. The sample was then rotated so that the signal propagated perpendicular to the fiber orientation in the sample (Fig. 3b). Again, the main bang and first echo were captured, and the longitudinal speed of sound perpendicular to the fiber orientation, $C_{L\perp}$, was calculated. The acoustic impedance was calculated both parallel and perpendicular to the fiber orientation as the product of ρ and the longitudinal speed of sound in each fiber orientation. The CFR PEEK samples were measured twice for each orientation with the transducer coupled first to one face of the sample and then to the opposite face for the second measurement.

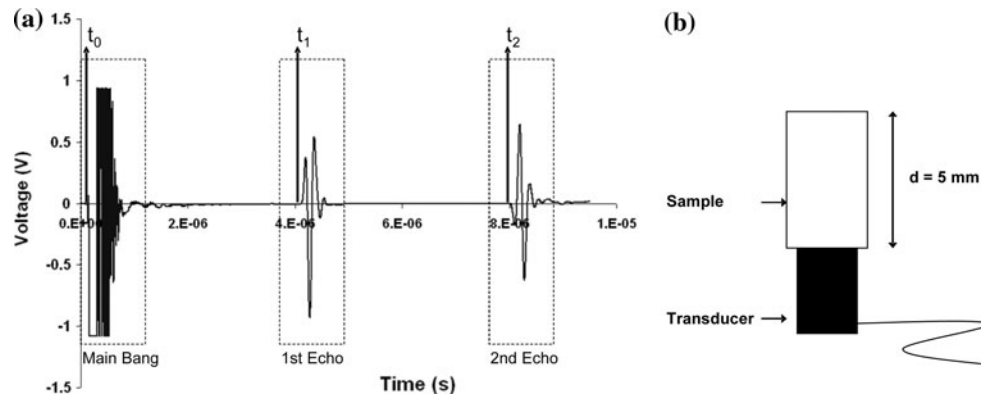


Fig. 2 Main bang and its first two echoes (a). The beginning of the main bang, t_0 , the first echo, t_1 , and the second echo, t_2 , are labeled. The distance traveled is equal to twice the length, d , of the sample,

since the signal travels the length of the sample, reflects off the opposite face of the sample, and then returns to the transducer (b)

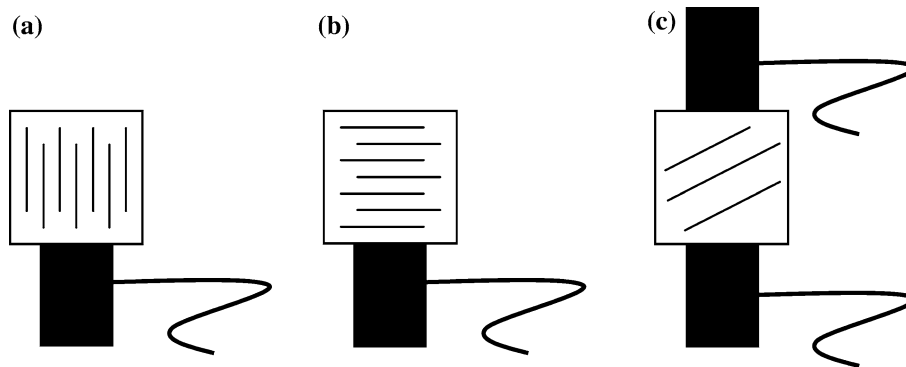


Fig. 3 Sample A was placed on the transducer so that the signal propagated parallel to the fiber orientation to measure $C_{L\parallel}^{\parallel}$ (a). Sample A was placed on the transducer so that the signal propagated

perpendicular to the fiber orientation to measure $C_{L\perp}^{\perp}$ (b). Sample D was placed between two transducers in through-transmission mode to measure C_{L77° (c)

Longitudinal couplant was applied to both sides of sample D from each dog-bone specimen. The sample was placed between two longitudinal transducers and connected to the pulser–receiver in through-transmission mode (Fig. 3c). This configuration allowed measurements to be performed at 77° relative to the fiber direction of the sample, where 0° is parallel to the fiber direction and 90° is perpendicular. The main bang and the signal that reached the second transducer were captured. The speed of sound, C_{L77° , was calculated the same way as described above except the distance traveled was only one length of the specimen. Each CFR PEEK sample was measured twice along the 77° orientation by interchanging the faces to which the transmitting and receiving transducers were coupled.

Transverse couplant was applied to both sides of sample A from each dog-bone specimen. The sample

was placed between two transverse transducers so that the signal was polarized perpendicular to the fiber axis and the propagation was parallel to the fiber axis. The main bang and the signal that reached the second transducer were captured. The speed of sound polarized perpendicular and propagating parallel to the fiber orientation, $C_{T\perp}^{\parallel}$, was calculated. The sample was rotated so that the signal was polarized perpendicular to the fiber axis and the propagation was perpendicular to the fiber axis. Again, the main bang and the signal that reached the second transducer were captured. The speed of sound polarized perpendicular and propagating perpendicular to the fiber orientation, $C_{T\perp}^{\perp}$, was then calculated. The CFR PEEK samples were measured twice for each polarization and propagation direction by interchanging the faces to which the transmitting and receiving transducers were coupled.

Mechanical properties

PEEK mechanical properties

In order to determine the mechanical properties of PEEK, Eqs. 2–5 were solved using the values of C_L , C_T , and ρ found during the speed of sound measurements [3]. These equations were solved to find Poisson’s ratio (ν), Young’s modulus (E), shear modulus (G), and bulk modulus (K), respectively.

$$\nu = \frac{(C_L^2 - 2C_T^2)}{2(C_L^2 - C_T^2)} \tag{2}$$

$$E = 2\rho C_T^2(1 + \nu) \tag{3}$$

$$G = \frac{E}{2(1 + \nu)} \tag{4}$$

$$K = \frac{E}{3(1 - 2\nu)} \tag{5}$$

CFR PEEK mechanical properties

The procedure for calculating the mechanical properties of a unidirectional fiber-reinforced composite material is summarized below. The elastic stiffness matrix for such a material has six independent stiffness coefficients, namely c_{11} , c_{33} , c_{44} , c_{66} , c_{12} , and c_{13} . The matrix coefficients were calculated by solving Eqs. 6–13 using values of $C_{L\parallel}^{\parallel}$, $C_{L\perp}^{\perp}$, C_{L77° , $C_{T\perp}^{\parallel}$, $C_{T\perp}^{\perp}$, and ρ obtained during the speed of sound measurements. The coefficient c_{13} is determined from the longitudinal speed of sound measured at some angle relative to the fiber direction between 0° and 90° . Traditionally 45° is used; however, an angle of 77° was chosen for this study because it has been shown to minimize the error when calculating the coefficient c_{13} [4]. The compliance matrix was obtained by inverting the stiffness matrix shown in Eq. 14. Equation 15 shows the compliance matrix and how the values of Young’s modulus (E), shear modulus (G), and Poisson’s ratio (ν) were calculated along each axis of the CFR PEEK samples (Fig. 4).

$$c_{11} = \rho (C_{L\perp}^{\perp})^2, \tag{6}$$

$$c_{33} = \rho (C_{L\parallel}^{\parallel})^2, \tag{7}$$

$$c_{44} = \rho (C_{T\perp}^{\parallel})^2, \tag{8}$$

$$c_{66} = \rho (C_{T\perp}^{\perp})^2, \tag{9}$$

$$c_{12} = c_{11} - 2c_{66}, \tag{10}$$

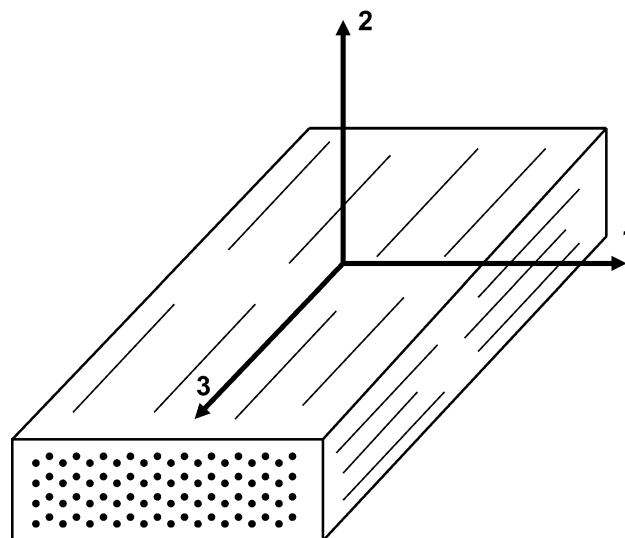


Fig. 4 The coordinate system with respect to the fiber orientation of the CFR PEEK samples. Axes 1 and 2 are perpendicular to the fiber axis, while axis 3 is parallel to the fiber axis

$$a = c_{11} \sin^2 77^\circ + c_{33} \cos^2 77^\circ + c_{44} \tag{11}$$

$$b = (c_{33} \cos^2 77^\circ + c_{44} \sin^2 77^\circ) \times (c_{11} \sin^2 77^\circ + c_{44} \cos^2 77^\circ) \tag{12}$$

$$c_{13} = \frac{\sqrt{b - a\rho (C_{L77^\circ})^2 + \rho^2 (C_{L77^\circ})^4}}{|\sin 77^\circ| |\cos 77^\circ|} - c_{44} \tag{13}$$

$$c_{ij} = \begin{bmatrix} c_{11} & c_{12} & c_{13} & 0 & 0 & 0 \\ c_{12} & c_{11} & c_{13} & 0 & 0 & 0 \\ c_{13} & c_{13} & c_{33} & 0 & 0 & 0 \\ 0 & 0 & 0 & c_{44} & 0 & 0 \\ 0 & 0 & 0 & 0 & c_{44} & 0 \\ 0 & 0 & 0 & 0 & 0 & c_{66} \end{bmatrix} \tag{14}$$

$$s_{ij} = c_{ij}^{-1} = \begin{bmatrix} \frac{1}{E_1} & -\frac{\nu_{12}}{E_2} & -\frac{\nu_{13}}{E_3} & 0 & 0 & 0 \\ -\frac{\nu_{21}}{E_1} & \frac{1}{E_2} & -\frac{\nu_{23}}{E_3} & 0 & 0 & 0 \\ -\frac{\nu_{31}}{E_1} & -\frac{\nu_{32}}{E_2} & \frac{1}{E_3} & 0 & 0 & 0 \\ 0 & 0 & 0 & \frac{1}{G_{23}} & 0 & 0 \\ 0 & 0 & 0 & 0 & \frac{1}{G_{13}} & 0 \\ 0 & 0 & 0 & 0 & 0 & \frac{1}{G_{12}} \end{bmatrix} \tag{15}$$

The values of E_1 , E_2 , and E_3 are the Young’s modulus along axes 1, 2, and 3, respectively. The Young’s modulus was found at other angles by rotating the coordinate system. This process is described in the literature, and is summarized briefly here [5]. In order to rotate from the original coordinate system, x_i , to a new coordinate system, x_i' , a 3×3 transformation matrix, M_{ij} , is defined as shown in Eq. 16.

$$[M_{ij}] = \begin{bmatrix} a_{11}^2 & a_{12}^2 & a_{13}^2 & 2a_{12}a_{13} & 2a_{13}a_{11} & 2a_{11}a_{12} \\ a_{21}^2 & a_{22}^2 & a_{23}^2 & 2a_{22}a_{23} & 2a_{23}a_{21} & 2a_{21}a_{22} \\ a_{31}^2 & a_{32}^2 & a_{33}^2 & 2a_{32}a_{33} & 2a_{33}a_{31} & 2a_{31}a_{32} \\ a_{21}a_{31} & a_{22}a_{32} & a_{23}a_{33} & a_{22}a_{33} + a_{23}a_{32} & a_{21}a_{33} + a_{23}a_{31} & a_{22}a_{31} + a_{21}a_{32} \\ a_{31}a_{11} & a_{32}a_{12} & a_{33}a_{13} & a_{12}a_{33} + a_{13}a_{32} & a_{13}a_{31} + a_{11}a_{33} & a_{11}a_{32} + a_{12}a_{31} \\ a_{11}a_{21} & a_{12}a_{22} & a_{13}a_{23} & a_{12}a_{23} + a_{13}a_{22} & a_{13}a_{21} + a_{11}a_{23} & a_{11}a_{22} + a_{12}a_{21} \end{bmatrix} \quad (16)$$

The components of this matrix are the direction cosines given in Eq. 17.

$$a_{ij} = \cos(x'_i, x_j) \quad (17)$$

Using the Bond rotation equation, Eq. 18, the rotated elastic stiffness matrix, c_{ij}' , is found. This matrix is inverted to obtain a new compliance matrix, and the Young's modulus is calculated using Eq. 15. In order to demonstrate the utility of Bond rotations, we performed Bond rotations around axis 2 in 2° increments of the CFR PEEK samples to determine Young's modulus at each angle. The shear modulus and Poisson's ratio at other angles can be found in the same manner.

$$[c'_{ij}] = [M_{ij}] [c_{ij}] [M_{ij}]^T \quad (18)$$

Broadband ultrasound attenuation

PEEK broadband ultrasound attenuation

In order to calculate the BUA, the first and second longitudinal echoes were captured for each PEEK sample as shown in Fig. 2. The first echo was centered within a 4-μs Hanning window, and a fast Fourier transform (FFT) was performed resulting in a power spectrum $P_1(f)$. This was repeated for the second echo. A log spectral subtraction was used to obtain signal loss in decibels as a function of frequency as shown in Eq. 19. A line was fit to the signal loss spectrum over the 10-dB bandwidth of the power spectrum of the second echo. The 10-dB bandwidth was slightly different for each sample, but normally ranged from 3 to 7 MHz. The slope of this regression line in units of dB/MHz was divided by twice the length of the specimen, $2d$, in centimeters for a BUA value in units of dB/cm MHz. BUA measurements were performed twice for each of the seven PEEK samples with the transducer coupled first to one face of the sample and then to the opposite face for the second trial. Transverse BUA was also calculated for each PEEK sample using a similar procedure except with transverse echoes.

$$\text{Signal Loss} = 10 \log_{10} P_1(f) - 10 \log_{10} P_2(f) \quad (19)$$

CFR PEEK broadband ultrasound attenuation

The longitudinal BUA was determined both parallel and perpendicular to the fiber axis of the CFR PEEK samples. In order to determine BUA parallel to the fiber direction, the first longitudinal echo parallel to the fiber orientation was obtained for sample A of each specimen. Then, the first longitudinal echo parallel to the fiber orientation was obtained for sample B of each specimen. The BUA analysis described above was repeated by performing a log spectral subtraction of sample B from sample A to obtain the signal loss spectrum using Eq. 19. A line was fit to this curve, and the resulting slope was divided by twice the difference in length between samples A and B to determine BUA. In order to determine BUA perpendicular to the fiber direction, the first and second longitudinal echoes perpendicular to the fiber axis were obtained for sample C of each specimen. The BUA perpendicular to the fiber axis was then calculated in a similar manner except that the slope of the signal loss spectrum was divided by twice the length of sample C.

Results

Speed of sound measurements

The longitudinal and transverse speeds of sound values in PEEK were 2536 ± 10 and 1086 ± 6 m/s, respectively. The speeds of sound values for CFR PEEK are listed in Table 1. The values reported for speed of sound represent the mean and standard deviation of 14 measurements

Table 1 Average speed of sound values for CFR PEEK

$C_{L }^ $ (m/s)	$C_{L\perp}^{\perp}$ (m/s)	C_{L77° (m/s)	$C_{T\perp}^ $ (m/s)	$C_{T\perp}^{\perp}$ (m/s)
4917 ± 21	2693 ± 16	2857 ± 19	1325 ± 6	1223 ± 7

(seven samples, two trials each). The densities for the PEEK and CFR PEEK samples were 1285 ± 3 and 1331 ± 14 kg/m³, respectively. These density values represent the mean and standard deviation of seven samples (one measurement per sample). The acoustic impedances was 3.26 ± 0.01 MPa s/m for PEEK. The acoustic impedance measured parallel and perpendicular to the fiber orientation of the CFR PEEK were 6.57 ± 0.08 and 3.59 ± 0.03 MPa s/m, respectively.

Mechanical properties

PEEK mechanical properties

Table 2 shows the mechanical properties of PEEK calculated using speed of sound measurements. Since the PEEK

Table 2 Average mechanical properties of PEEK

<i>E</i> (GPa)	<i>G</i> (GPa)	<i>K</i> (GPa)	ν
4.21 ± 0.04	1.52 ± 0.01	6.25 ± 0.05	0.388 ± 0.001

Table 3 Average mechanical properties of CFR PEEK

<i>E</i> (GPa)		<i>G</i> (GPa)		ν		
<i>E</i> ₁ , <i>E</i> ₂	<i>E</i> ₃	<i>G</i> ₁₃ , <i>G</i> ₂₃	<i>G</i> ₁₂	ν ₁₂ , ν ₂₁	ν ₁₃ , ν ₂₃	ν ₃₁ , ν ₃₂
4.80 ± 0.36	15.0 ± 2.3	2.3 ± 0.1	1.96 ± 0.05	0.25 ± 0.06	0.78 ± 0.08	0.31 ± 0.05

samples were isotropic, the mechanical properties are constant regardless of the orientation of the material.

CFR PEEK mechanical properties

Table 3 shows the Young’s modulus, shear modulus, and Poisson’s ratio values for the coordinate system used in Fig. 4. Figure 5 shows the angular dependence of Young’s modulus for the CFR PEEK samples in both the meridian and transverse planes obtained by performing a Bond rotation of the coordinate system as described earlier. The meridian plane is defined as the 1–3 plane (Fig. 4). The transverse plane is defined as the 1–2 plane.

Broadband ultrasound attenuation

The longitudinal, *BUA_L*, and transverse, *BUA_T*, *BUA* values for PEEK are shown in Table 4. Also shown are the longitudinal *BUA* parallel, *BUA_{L||}*, and perpendicular, *BUA_{L⊥}*, to the fiber orientation of the CFR PEEK samples.

Fig. 5 Polar plots showing the angular dependence of Young’s modulus for the CFR PEEK samples in the meridian (a) and transverse (b) planes

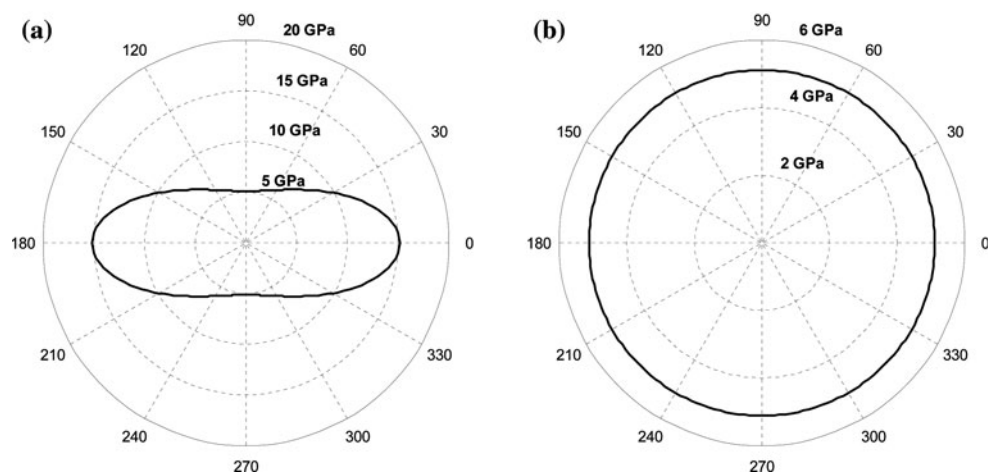


Table 4 *BUA* values for PEEK and CFR PEEK

PEEK <i>BUA_L</i> (dB/cm MHz)	PEEK <i>BUA_T</i> (dB/cm MHz)	CFR PEEK <i>BUA_L</i> (dB/cm MHz)	CFR PEEK <i>BUA_{L⊥}</i> (dB/cm MHz)
1.33 ± 0.14	4.37 ± 0.82	2.43 ± 1.0	1.45 ± 0.26

Discussion

Speed of sound measurements

PEEK speed of sound measurements

Rae et al. [3] reported both the longitudinal and transverse speeds of sound values for a known grade of PEEK, PEEK 450G. PEEK 450G is the older Victrex nomenclature for the same grade of PEEK used in this study. Table 5 compares C_L , C_T , ρ , and Z between the current study and those of Rae et al. We find differences between the two studies for these parameters of 2.1, 3.9, 1.8, and 5.0%, respectively. Our speed of sound measurements (C_L and C_T) are both lower than those reported by Rae et al. The small but systematic difference may be attributable to differences between measurement techniques or the material properties of the samples. Table 5 also compares Z to two studies that measured acoustic impedance in unidentified, non-reinforced grades of PEEK [6, 7]. The difference was 0.3 and 2.4%, respectively. The density found in the current study is only 1.1% different from the value of 1300 kg/m^3 reported in the specification sheet for PEEK Optima[®] LT1 [2].

CFR PEEK speed of sound measurements

A literature search produced no results for speed of sound values for this grade of CFR PEEK for direct comparison. The longitudinal speed of sound parallel to the fiber orientation is significantly larger than that perpendicular to the fiber orientation as is seen in other anisotropic materials with unidirectional fiber orientation [4]. Also, as expected, the transverse speed of sound values are smaller than the longitudinal speed of sound values. The average density of the CFR PEEK specimens was $1331 \pm 14 \text{ kg/m}^3$ which is only 4.9% different from the value of 1400 kg/m^3 reported in the specification sheet for PEEK Optima[®] LT1CA30 [8].

Mechanical properties

PEEK mechanical properties

Table 6 shows how the mechanical properties of PEEK from this study compared with previously reported values.

Table 5 Comparison of average speed of sound in PEEK

	C_L (m/s)	C_T (m/s)	ρ (kg/m^3)	Z (MPa s/m)
Current study	2536.3	1086.1	1286	3.22
Rae 2007	2590	1130	1310	3.39
Millet 2004	–	–	–	3.21
Carlson 2003	–	–	–	3.30
PEEK optima [®] LT1	–	–	1300	–

Table 6 Comparison of mechanical properties with previously reported values

	E (GPa)	G (GPa)	K (GPa)	ν
Current study	4.2	1.5	6.2	0.388
Rae 2007 (ultrasonic)	4.6	1.7	6.6	0.380
Rae 2007 (mechanical)	4.1	–	–	–
Sandler 2002	4.0	–	–	–
PEEK optima [®] LT1	–	1.3	–	0.4

When compared to the Young's modulus, shear modulus, bulk modulus, and Poisson's ratio measured using speed of sound values reported by Rae et al., the differences were 8.7, 11.7, 6.1, and 2.1%, respectively [3]. Rae also measured the Young's modulus mechanically as 4.1 GPa, which is 2.4% different from the current value. Sandler et al. mechanically measured the Young's modulus of PEEK to be 4.0 GPa, which is 5.0% different from the current value [9]. The current values were also compared to the shear modulus and Poisson's ratio listed in the Invibio PEEK Optima[®] LT1 specification sheet [2]. When compared with the properties specified by the Invibio specification sheet, the difference in shear modulus and Poisson's ratio were 15.4 and 3.0%, respectively.

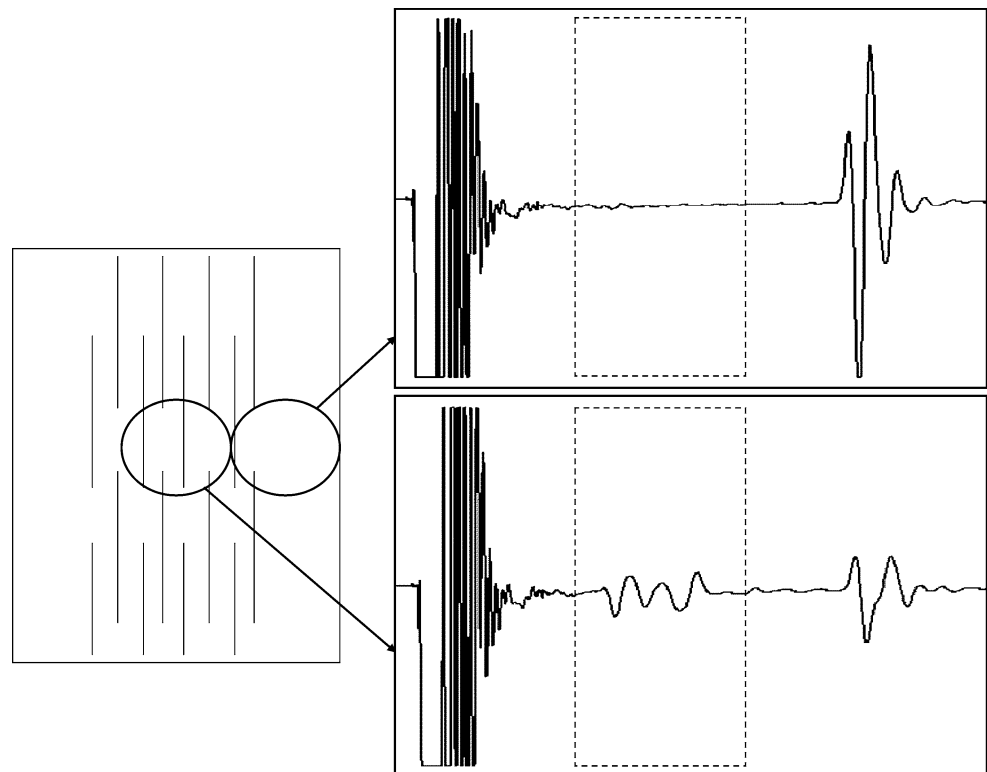
CFR PEEK mechanical properties

The Young's moduli parallel and perpendicular to the fiber orientation of the CFR PEEK samples were reported in the PEEK Optima[®] LT1CA30 specification sheet as 15.0 and 9.9 GPa, respectively [8]. The current values parallel, E_3 , and perpendicular, E_1 and E_2 , to the fiber orientation were 15.1 and 5.1 GPa. This marked a difference of 0.7 and 48.5%, respectively.

One possible reason for the large discrepancy in values for Young's modulus perpendicular to the fiber direction is the fact that the samples are molded with the carbon fibers flow distributed through the tensile bars instead of cut into dog-bone shapes from a sheet of the material. During speed of sound measurements, it was discovered that the fibers were concentrated in the center of the samples with fewer fibers in the areas near the edges of the bar. Figure 6 shows two longitudinal transducer placements represented by circles with the system operating in pulse–echo mode. The right placement is above the area immediately adjacent to the edge of the sample. The middle placement is above the center of the sample where the carbon fibers are concentrated. The graphs show the resulting echoes from the two transducer placements.

The main bang and first echo are shown in the top graph of Fig. 6 as the signal travels through the material with low fiber concentration, reflects off the opposing surface, and

Fig. 6 The carbon fibers were not uniformly distributed throughout the CFR PEEK tensile bars. The circles represent longitudinal transducer placements on the sample, and the graphs show the longitudinal echoes resulting from each placement



returns to the transducer. The bottom graph of Fig. 6 shows the main bang and first echo, but with smaller secondary echoes between them, shown in the dotted box. These secondary echoes may result from the sound waves back-scattering from the carbon fibers and returning to the transducer. In addition, the echo from the opposite face of the specimen in the bottom graph of the figure is noticeably attenuated compared to that in the top graph. This also indicates that the fiber concentration is greater in the center of the samples. This uneven distribution of carbon fibers does not affect strongly our measured values of Young's modulus parallel to the fiber orientation because the ultrasonic wave propagates mainly in the region of high fiber concentration. However, for measurements made perpendicular to the fiber direction, the wave travels through regions of high and low fiber concentration.

Figure 5 shows the angular dependence of Young's modulus for CFR PEEK in both the meridian and transverse planes. In the meridian plane, the Young's modulus is anisotropic with a maximum value of 15.1 GPa occurring at 0° and 180° and a minimum value of 5.1 GPa at 90° and 270° . As expected, the maximum values coincide with angles that are aligned with the fiber orientation and the minimum values occur at angles that are perpendicular to the fiber orientation. In the transverse plane, the Young's modulus is isotropic with a value of 5.1 GPa.

Broadband ultrasound attenuation

There are only two reported values of longitudinal ultrasound attenuation in PEEK, both at 5 MHz [7, 10]. There is no consensus between the two studies with one reporting the ultrasound attenuation at 20°C as 52.29 Np/m and the other approximately 35 Np/m [7, 10]. The studies also show conflicting data as to the effects of temperature on ultrasound attenuation. Carlson reports that ultrasound attenuation decreases with an increase in temperature, and Van Deventer reports the opposite. By evaluating our measured longitudinal BUA at 5 MHz and converting from dB/cm to Np/m we obtain a value 76.6 Np/m for the ultrasonic attenuation of PEEK at 5 MHz.

The longitudinal BUA of PEEK was estimated as 0.955 dB/cm MHz from the slope of the attenuation versus frequency graph reported by Carlson between 4 and 6.5 MHz [7]. This value is almost 40% less than our value of 1.33 dB/cm MHz. The longitudinal BUA of PEEK could not be estimated from the Van Deventer's study.

There are several possible reasons for differences in the results. The first is a difference in the method of testing. Carlson performed their studies by submerging their samples in an ultrasonic water tank, while in this study the samples were placed directly on the transducers. Second, the current longitudinal BUA was calculated over a 10-dB

broadband instead of the 6-dB broadband used in the Carlson study. Lastly, these measurements are very sensitive to the reflective surfaces of the samples being parallel. It is possible some error is introduced if the sample surfaces are not exactly parallel. We tried to minimize this effect as much as possible when preparing the samples by using a lathe to machine faces of the specimens.

There are no published values of transverse BUA values of PEEK, but as expected the current results show significantly greater attenuation for the transverse measurements when compared to the longitudinal measurements. These values are of use when calculating or modeling the effects of ultrasound on PEEK. The few studies which have investigated the ultrasonic attenuation of PEEK have focused on longitudinal attenuation. The transverse attenuation must also be taken into account when used in modeling. When a longitudinal wave is incident upon an interface, it can partially mode convert to a transverse wave if the angle of incidence is non-perpendicular.

Likewise, there are no published values of longitudinal BUA in CFR PEEK. We find that the BUA parallel to the fiber direction is less than the BUA perpendicular to the fiber direction. Greater attenuation perpendicular to the fibers is expected and may be related in part to the lower speed of sound along this direction.

Experimental errors

Most of the measured values reported in this study are presented in the form of mean \pm standard deviation where the mean and standard deviation are determined from multiple measurements on multiple samples of PEEK and CFR PEEK. The standard deviation reflects random measurement errors and random variations between samples. In the case of CFR PEEK, measurements may also depend on the specific site that is ultrasonically interrogated. As described earlier, there is evidence that the carbon fibers may not be distributed evenly throughout a given sample.

The experimental error in the speed of sound measurements may be estimated by summing the percent error in the timing measurements and in the length measurements of the specimens. We estimate an uncertainty of 0.02 μ s in the timing measurements and an uncertainty of 0.2 mm in the length measurements. The shortest measured time interval ($t_1 - t_0$ in Eq. 1) was approximately 4 μ s. The shortest specimen length was 5 mm. Thus, the estimated maximum uncertainty in the speed of sound measurements reported in this study is 4.5%.

It is more difficult to estimate the experimental error in BUA because of the complicated nature of the signal analysis that is involved. Experimentally, BUA measurements are more difficult to perform than speed of sound measurements because BUA is very sensitive to the

alignment of the sample with the transducer(s). Slight misalignment can produce phase cancellation effects at the face of a phase sensitive receiving transducer. The experimental challenges associated with measuring BUA are reflected in the standard deviations reported in Table 4. The coefficients of variation (mean divided by standard deviation) range between 11 and 41%. This compares to less than 1% for the speed of sound measurements.

Limitations

Ultrasonic techniques offer a useful nondestructive approach for evaluating the viscoelastic properties of materials. However, it should be noted that there are fundamental differences between ultrasonic and conventional mechanical testing techniques. In particular, ultrasonic techniques produce much smaller strains at much higher strain rates. While the mechanical moduli measured in this study by ultrasonic techniques compare well with mechanical moduli measured by conventional mechanical testing, exact agreement between the two techniques generally is not expected.

All measurements reported in this study were performed at room temperature. However, the properties of PEEK and CFR PEEK may be different at body temperature (37 °C). Carlson et al. measured the ultrasonic properties of PEEK at 5, 20, and 37 °C using 5- and 10-MHz transducers [7]. At 5 MHz, they found a 1.2% decrease in the speed of sound and a 16% decrease in the attenuation coefficient. There are no reported measurements of the temperature dependence of the ultrasonic properties of CFR PEEK in the literature. However, the temperature dependent mechanical properties of CFR PEEK (PEEK/IM7) have been reported by Jeyaraj et al. [11]. When the temperature was increased from 20 to 40 °C, no changes were observed in Poisson's ratio and Young's modulus perpendicular to the fiber orientation. Young's modulus parallel to the fiber direction decreased by 0.13% and the shear modulus decreased by 1.4%. In addition, they reported a "system loss factor" associated with the vibrational damping of a square plate of CFR PEEK. The loss factor was found to increase by as much as 8.5%, when the temperature was increased from 20 to 40 °C. This finding suggests that the ultrasonic attenuation of CFR PEEK may increase with temperature.

Conclusions

This study evaluates the mechanical properties of PEEK and CFR PEEK using nondestructive, ultrasonic techniques. The Young's modulus of CFR PEEK is fully characterized with respect to fiber orientation in both the meridian and transverse planes. This study highlights the

use of a nondestructive, ultrasonic evaluation method that can be used to evaluate not only the Young's modulus, but also the shear modulus and Poisson's ratio, of any, unidirectional fiber-reinforced material. In addition, the longitudinal and transverse broadband ultrasound attenuations of PEEK are reported. The longitudinal broadband ultrasound attenuations of CFR PEEK both parallel and perpendicular to the fiber orientation are also reported. These are the first reports of transverse BUA in PEEK and longitudinal BUA in CFR PEEK.

Acknowledgements The authors would like to thank Mr. Glen Davis for his assistance with the preparation of specimens, and Dr. Scott Handley for useful discussions relating to data analysis.

References

1. Kurtz SM, Devine JN (2007) *Biomaterials* 28:4845
2. PEEK Optima[®] LT1 typical material properties. Invibio Ltd., Thornton Cleveleys, Lancashire, UK
3. Rae PJ, Brown EN, Orler EB (2007) *Polymer* 48:598
4. Handley SM (1992) Physical principles pertaining to ultrasonic and mechanical properties of anisotropic media and their application to nondestructive evaluation of fiber-reinforced composite materials. Dissertation, Washington University, St. Louis, MO, May, 1992.
5. Hoffmeister BK, Smith SR, Handley SM, Rho JY (2000) *Med Biol Eng Comput* 38:333
6. Millett JCF, Bourne NK, Gray GT (2004) *J Phys D Appl Phys* 37:942
7. Carlson JE, van Deventer J, Scolan A, Carlander C (2003) Frequency and temperature dependence of acoustic properties of polymers used in pulse-echo systems. In: *IEEE Ultra Symposium 2003*, pp 885–888
8. PEEK Optima[®] LT1CA30 typical material properties. Invibio Ltd., Thornton Cleveleys, Lancashire, UK
9. Sandler J, Werner P, Shaffer MSP, Demchuk V, Altstadt V, Windle AH (2002) *Compos A* 33:1033
10. van Deventer J, Lofqvist T, Delsing J (2000) *IEEE Trans Ultra Ferr Freq Con* 47:1014
11. Jeyaraj P, Ganesan N, Padmanabhan C (2009) *J Sound Vib* 320:322